Synthesis, Optical and Electrochemical Properties of Isomeric Dibenzophenanthroline Derivatives

Animesh Ghosh,[a] Tianjiao Li,[b] Wenjun Ni,[b] Tong Wu,[b] Caihong Liang,[a] Maja Budanovic,[c] Samuel A. Morris,[a] Maciej Klein,[d] Richard D. Webster,[c] Gagik G. Gurzadyan,*[b] and Andrew C. Grimsdale*[a]

[a] School of Materials Science and Engineering, Nanyang Technological University, 50 Nanyang Avenue, Singapore 639798

[b] Institute of Artificial Photosynthesis, State Key Laboratory of Fine Chemicals, Dalian University of Technology, 2 Ling Gong Road, Dalian 116024, China

[c] Division of Chemistry and Biological Chemistry, School of Physical and Mathematical Sciences, Nanyang Technological University, 21 Nanyang Link, Singapore 637371

[d] Division of Physics and Applied Physics, School of Physical and Mathematical Sciences, Nanyang Technological University, 21 Nanyang Link, Singapore 637371.

* Corresponding authors: gurzadyan@dlut.edu.cn; acgrimsdale@ntu.edu.sg

Abstract: Acid catalysed Friedländer cyclization of 2-aminobenzophenones with 1,2-, 1,3-, and 1,4-cyclohexadiones, followed by aromatization, has been used to prepare dibenzophenanthrolines (DBPs) containing 1,10-, 1,7- and 4,7-phenanthroline units, whose optoelectronic properties have been compared. The LUMO energies for all isomers were similar but the 4,7-isomers possessed significantly higher HOMOs than the other isomers, resulting in them having smaller HOMO-LUMO energy gaps. Compared with 1,10-DBP isomers, the emission of 1,7-DBPs is strongly quenched due to efficient charge transfer. The 4,7-DBP isomers show strongly enhanced photoluminescence due to excimer formation but

appear to be less photostable due to their higher HOMO levels. Bis(phenylethynyl)-substituted derivatives demonstrated improved solubility and stronger luminescence properties than their unsubstituted analogues.

Introduction

Extended π-conjugated planar organic molecules with fused rings such as acenes are of great research interest because of their potential application in organic field effect transistors (OFETs), organic light emitting diodes (OLEDs) and organic photovoltaic devices (OPVs).[1] Although exceptionally high charge carrier mobilities (>10 cm^2 V^{-1} s^{-1}) have been measured in single crystals of pentacene (**1**) (**Figure 1**) and other acene derivatives such as rubrene, which are higher than in some silicon-based devices, their practical usefulness in organic electronic devices is restricted due to their low stability towards air and for unsubstituted acenes, their low solubility in common organic solvents.[2]

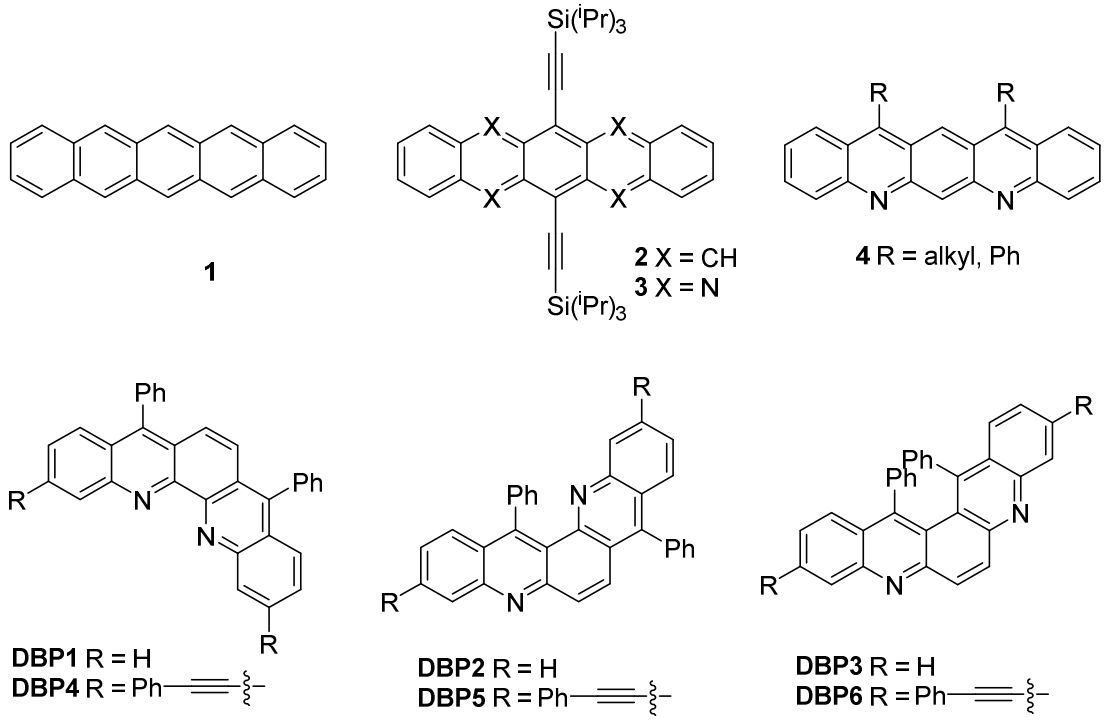

Figure 1. Chemical structures of acenes and heteroacenes.

Incorporation of electronegative heteroatoms such as nitrogen into acenes allows fine-tuning of electronic properties, may enhance intermolecular interaction and increase electron mobilities.[3] Some heteroacenes such as **3** have been reported to possess high electron mobilities. A great deal of research effort has been dedicated in recent years into designing heteroacenes having high air stability, good solubility and high charge carrier mobility. The stability of linear heteroacenes diminishes with the increasing of molecular length and in some cases results in decomposition of the molecule.[3k, 4] However nonlinear heteroacenes of higher molecular length are reported to be more stable due to their greater number of aromatic rings with filled sextets. Therefore, although most attention has been directed towards linear heteroacenes, recently there have been some reports on the synthesis and investigation of nonlinear heteroacenes as organoelectronic materials.[3j, 5] Other research groups have developed nonlinear heteroacenes with optical and electronic properties suitable for applications including organic light emitting devices (OLED), organic field effect transistors (OFET) and organic photovoltaic devices (OPVs).[5b, 5e, 6]

In previous work we have developed routes to analogues of 5,7-diazapentacene,[7] and made some studies of their optoelectronic properties but these were found to be prone to formation of butterfly dimers during X-ray diffraction experiments, suggesting they have stability problems. It was hypothesised that nonlinear heteroacenes having symmetrically placed pyridine rings might demonstrate higher optical and electronic properties and address the issues of atmospheric stability and poor solubility. In this paper, we report an efficient synthetic approach for three dibenzophenanthroline isomers (**DBP1-3, Scheme 1**) and their bis(phenylethynyl)-substituted analogues (**DBP4-6, Scheme 2**) via a Friedländer double condensation reaction and investigate the influence of molecular structures on their photophysical and electrochemical properties. **DBP1** and **DBP2** have been previously made in moderate yield by coupling of 2-aminobenzophenone (**1**) with 1,2- and 1,3-diiodobenzene

followed by acid-catalyzed condensation of the resulting ketones,[8] but **DBP3** has not been previously reported. A subsequent report of **DBP1** (made by a Friedländer double condensation reaction) showed it could be used as a metal complexing ligand for photosensitizer applications,[9] and similar applications should also be possible for the isomers. Introduction of bis(phenylethynyl) functionality onto the main heteroacene ring was intended to increase solubility and tune the optoelectronic properties of the heteroacenes by extending their conjugation length.

Results and Discussion

Synthesis and characterization

Our synthetic route for the preparation of **DBP1**, **DBP2** and **DBP3** is illustrated in **Scheme 1**. The key pentacyclic dihydrodibenzophenanthroline intermediates (**2**, **3** and **4**) for all three isomers were prepared by acid-catalysed Friedländer double condensation reaction.[10] Compound **2** has previously been made in similar yields by Friedländer double condensation between 2-aminobenzophenone (**1**) and 1,2-cyclohexanedione catalyzed by indium(III),[11] or by cerium(IV)[12] - our procedure avoids use of the expensive metal reagents. It has been reported that dehydrogenation of **2** to **DBP1** can be achieved in 55% yield by refluxing with 10% Pd/C in nitrobenzene, [9] but we were unable to obtain **DBP1** by this method, nor by refluxing **2** in xylene with 2,3-dichloro-5,6-dicyenobenzoquinone (DDQ). Thus, it was necessary to investigate alternative procedures for aromatization of **2**. It was found that refluxing a 1,2-dichloroethane solution of **2** with *N*-bromosuccinimide and a catalytic amount of benzoyl peroxide led to the formation of **DBP1** in 55% isolated yield. The reaction, which proceeds via bromination of the active methylene group of **2** followed by *in situ* dehydrobromination of the bromo intermediate, has previously been used for aromatisation of other polycyclic aromatic compounds.[13] Compound **3** has been previously made in 86%

yield by solvent-free microwave-assisted Friedländer condensation of an acridone with **1** and concentrated sulfuric acid.[14a] The acridone has been reportedly made by condensation of **1** with 1,3-cyclohexadione in 99-100% yield,[14b-d] producing an overall yield of **3** from **1** in 2 steps of 85-86% yield. Our synthesis is shorter and uses milder conditions, but has a lower yield (40%). The dehydrogenation of pentacyclic intermediates **3** and **4** were carried out by heating them with DDQ in xylene as has previously been reported for aromatization of other PAHs,[15] to provide **DBP2** and **DBP3** in 58% and 46% isolated yield respectively (**Scheme 1).**

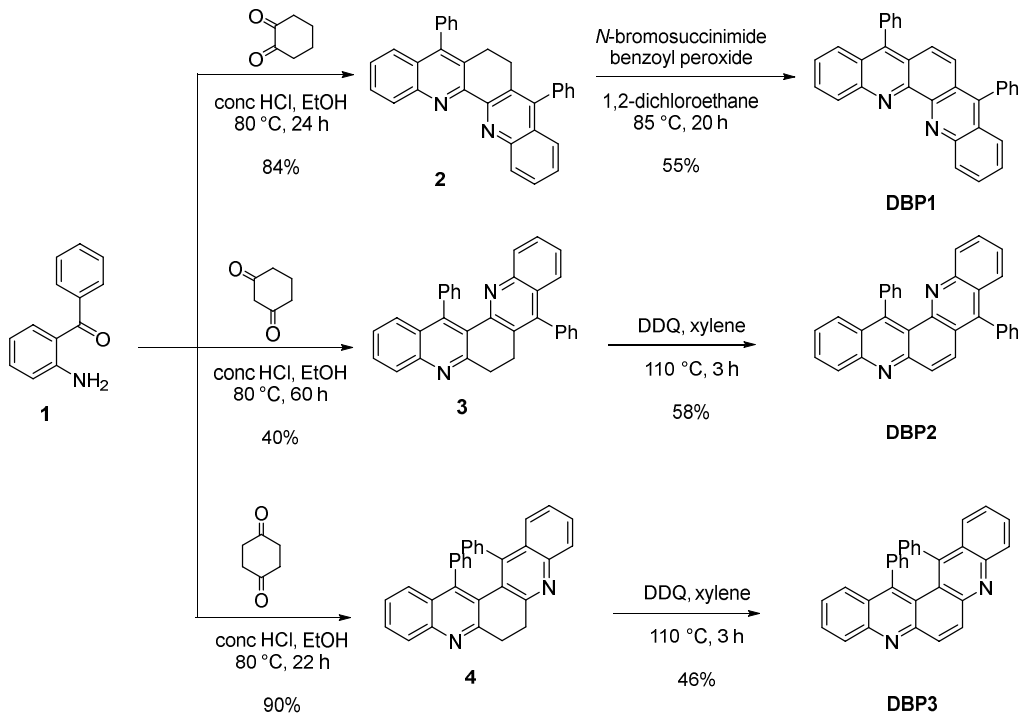

Scheme 1. Synthesis of Compounds **DBP1-3**

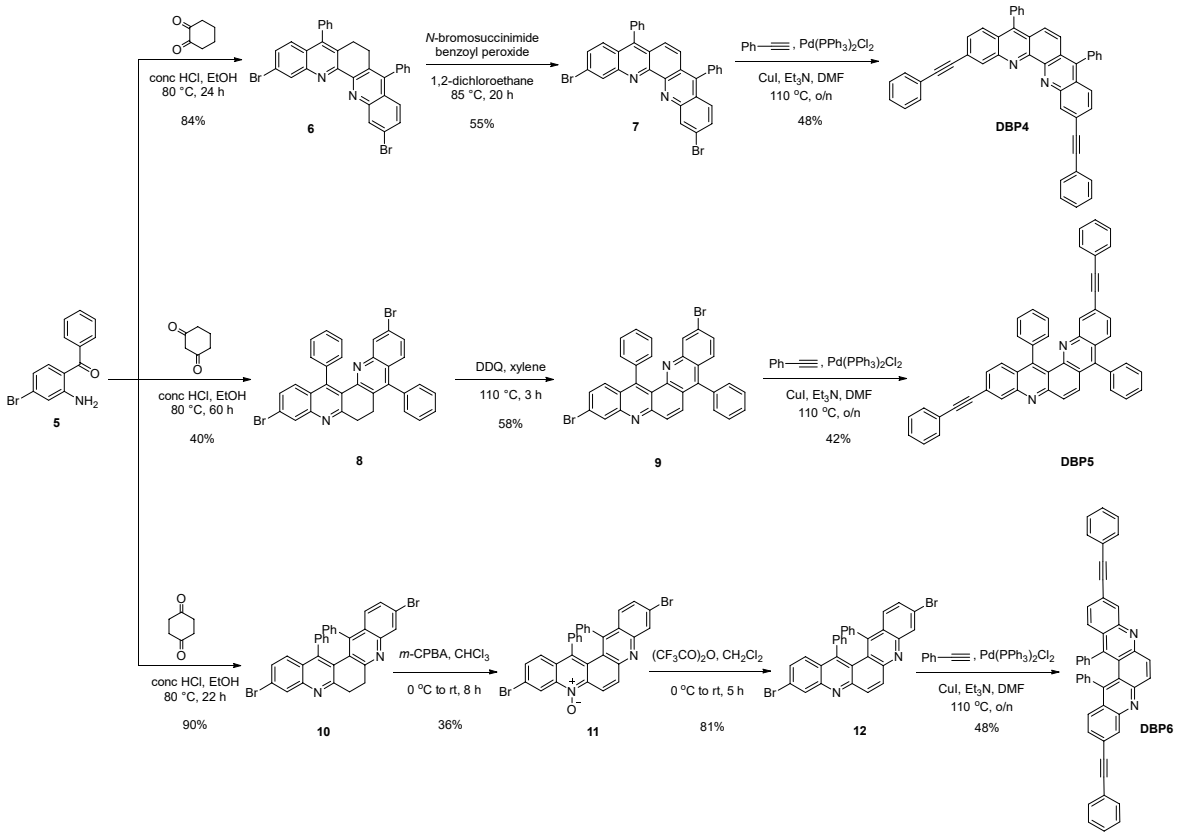

Scheme 2. Synthesis of compounds **DBP4-6**

The synthetic route for the preparation of bis(phenylethynyl)-substituted dibenzophenanthrolines **DBP4**, **DBP5** and **DBP6** is outlined in **Scheme 2**. Acid-catalysed Friedländer condensation[10] between 2-amino-4-bromobenzophenone (**5**) and 1,2-, 1,3-, and 1,4- cyclohexanedione provided the three different pentacyclic isomers **6**, **8**, and **10**. The aromatization of 6,7-dihydrodibenzo[*b,j*][1,10]phenanthroline **6** was attained by refluxing a 1,2-dichloroethane solution with *N*-bromosuccinimide and catalytic amount of benzoyl peroxide to provide dibromodibenzo[*b,j*][1,10]phenanthroline **7** in moderate yield. Finally the intermediate **7** was subjected to Sonogashira coupling with phenylacetylene giving the desired compound **DBP4** in 48% yield.[16] Dibromodiphenyl-6,7-dihydrodibenzo[*b,j*][1,7]phenanthroline **8** was dehydrogenated by heating a solution of xylene with DDQ at 110 °C to provide 13,11-dibromo-8,14-diphenyldibenzo[*b,j*][1,7]phenanthroline **9** in 59% yield.[15] The dibromo intermediate **12** was

obtained from the dihydrodibenzo[*b,j*][4,7]phenanthroline **10** in a two-step procedure. In the first step **10** was treated with *m*-chloroperbenzoic acid (mCPBA) providing N-oxide intermediate **11** which was next treated with trifluoroacetic anhydride to produce the dibromodibenzo[*b,*j][4,7]phenanthroline intermediate **12**.[17] Finally, the intermediates **9** and **12** were subjected to Sonogashira coupling reaction using similar reaction conditions to those in the synthesis of **DBP4** to provide the desired bis(phenylethynyl) substituted dibenzophenanthroline isomers **DBP5** and **DBP6** in moderate yields. All structures were supported by NMR, and high-resolution mass spectroscopy and single crystal X-ray diffraction data was obtained for **DBP1** and **DBP2**. To date we have been unable to grow crystals of the other DBP isomers which are suitable for XRD analysis. A crystal of **4**, the precursor to **DBP3** was obtained but only diffracted out to 1.4 Å. The best resolved image (see Supporting Information) certainly supports the structure but the thermal parameters are not within acceptable standards.

X-Ray single crystal data

The final refinement for **DBP1** yielded a R_1 = 5.64% and a wR_2 = 12.98% and a *goodness-of-fit* parameter of 1.028, it crystallised into an orthorhombic *Pbca* cell of size a = 9.6723(6) Å, b = 20.3067(12) Å, c = 21.5776(10) Å, $\alpha = \beta = \gamma = 90°$, V = 4238.1(4) Å^3. The refined structure is made of single units (**Figure 2a**) that display π-π stacking through the aromatic backbone at a distance of ~3.56 Å (**Figure S1a**) between units. The stacked units form a herringbone pattern down the *z*-axis (**Figure S1a**), which when viewed from 'above' (along the *z*-axis), can be observed to be distinct columns that only interact through van der Waals forces (**Figure S1b**).

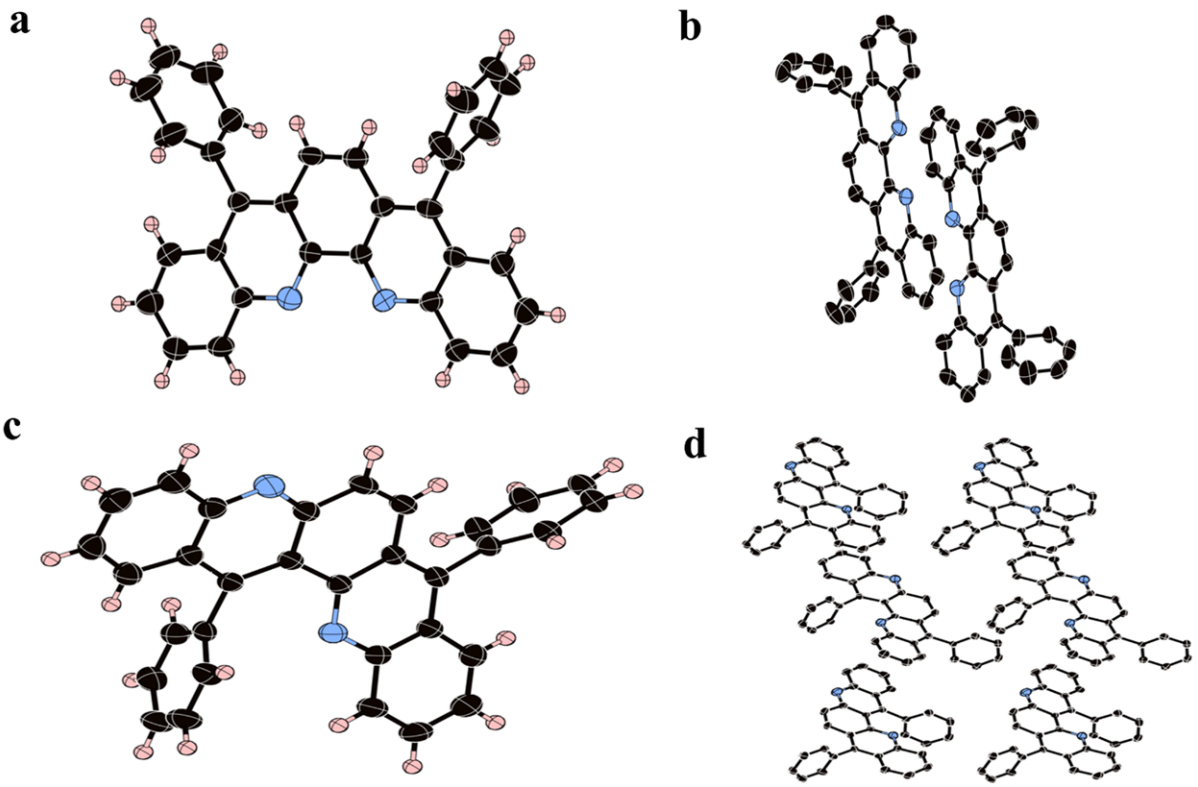

Figure 2a-d. X-ray crystal structure of **DBP1** (a) single molecule (b) molecules stacked. X-ray crystal structure of **DBP2** (c) single molecule (d) molecules stacked. All stacked structures are shown with hydrogen omitted for clarity. Black, blue and beige balls are carbon, nitrogen and hydrogen respectively. Probability density for thermal ellipsoids is 50%.

DBP2 crystallised into a monoclinic $P2_1/c$ (no. 14) cell of a = 10.4318(5) Å, b = 11.1646(6) Å, c = 18.5407(9) Å, β = 90.2770(10)°, V = 2159.35(19) Å^3. The final refinement R_1 = 3.74% and wR_2 = 9.32% with a *goodness-of-fit* parameter of 1.021. **Figure 2c** shows the single unit of **DBP2**. Unlike **DBP1**, **DBP2** does not stack to form a herringbone arrangement of layers, instead, all units arrange like fallen dominoes within a single layer, which stack in an ABAB arrangement that can be seen in **Figure 2d** and **Figure S1c**. Within each layer, the end aromatic unit display π-π stacking at a distance of ~3.65 Å, as shown using red arrows in

Figure 2d. π-π stacking does not occur between AB layers due to positional mismatch of the layers in the y-axis.

Electrochemical Properties of Compounds

The electrochemical behaviour of the dibenzophenanthroline isomers and bis(phenylethynyl) substituted dibenzophenanthrolines isomers were investigated by square-wave voltammetry (SWV) and cyclic voltammetry (CV) in dichloromethane (DCM) at room temperature with tetrabutylammonium hexafluorophosphate (Bu_4NPF_6) as the supporting electrolyte and using a glassy carbon (GC) working electrode. CV was used to study overall electrochemical behavior and SWV to determine oxidation/reduction potentials as it is a more sensitive technique for identifying redox processes. The redox potentials were determined relative to ferrocene/ferrocene$^+$ (Fc/Fc^+). The voltammograms obtained are shown in **Figures 3** and **4** and the data from these and from the SVW results are tabulated in **Table 1**.

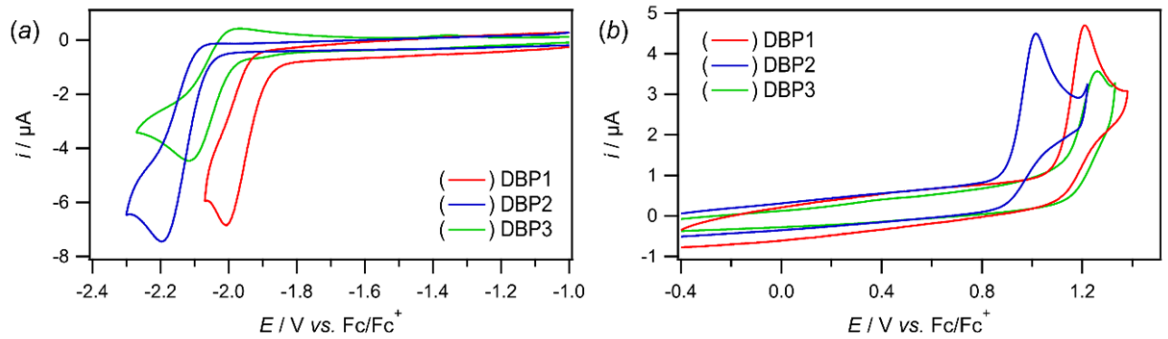

Figure 3. Comparison of (*a*) reduction and (*b*) oxidation process of 1 mM isomers (**DBP1**, **DBP2** and **DBP3**). Cyclic voltammograms were recorded in 0.1 M *n*Bu_4NPF_6/DCM at 0.1 V s^{-1} using 1 mm diameter GC working electrode at 298±2 K in a Faraday cage.

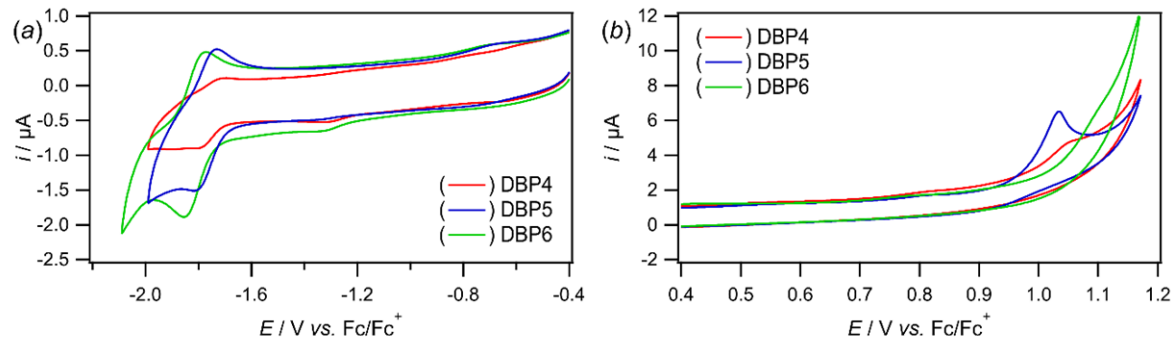

Figure 4. Comparison of (*a*) reduction and (*b*) oxidation process of 1 mM isomers (**DBP4**, **DBP5**, **DBP6**). Cyclic voltammograms were recorded in 0.1 M nBu$_4$NPF$_6$/DCM at 0.1 V s^{-1} using 1 mm diameter GC working electrode at 298±2 K in a Faraday cage.

As can be seen in **Figure 3,** the three dibenzophenanthroline isomers (**DBP1-3**) show chemically irreversible reduction and oxidation processes, indicating that their reduced and oxidized forms were relatively reactive. The CV behaviour of the bis(phenylethynyl)-substituted dibenzophenanthrolines isomers (**DBP4-6**) indicated that the compounds could be reduced and oxidized at similar potentials to the dibenzophenanthroline isomers. However, the reduction process of **DBP4, DBP5** and **DBP6** showed evidence of partial chemical reversibility since both a forward and reverse peak could be observed (**Figure 4a**) suggesting that the formed anion radicals survived on the CV timescale. By contrast, the first oxidation process of **DBP4**, **DBP5** and **DBP6** occurred at approximately +1.0 V *vs.* Fc/Fc$^+$ and all were chemically irreversible indicating rapid decomposition/reaction of the oxidised compounds (**Figure 4b**). The HOMO-LUMO values were calculated from the following equations and are tabulated in **Table 1**.[18]

$E_{HOMO} = -$ [E(onset, ox vs. Fc$^+$/ Fc) + 5.1](eV)

$E_{LUMO} = -$ [E(onset, red vs. Fc$^+$/ Fc) + 5.1](eV)

Table 1. Summary of electrochemical properties of compounds.

compound	E_{red} [V][a]	E_{ox} [V][a]	E_{onset}^{ox} [V]	E_{onset}^{red} [V]	HOMO [eV]	LUMO [eV]	E_g^{CV} [eV][b]
DBP1	-1.95	+1.20	+1.05	-1.85	-6.15	-3.25	2.90
DBP2	-2.15	+1.00	+0.85	-2.05	-5.95	-3.05	2.90
DBP3	-2.05	+1.25	+1.10	-1.95	-6.20	-3.15	3.05
DBP4	-1.80	+1.05	+0.95	-1.65	-6.05	-3.45	2.60
DBP5	-1.85	+1.00	+0.90	-1.70	-6.00	-3.40	2.60
DBP6	-1.75	+1.15	+1.00	-1.65	-6.10	-3.45	2.65

[a]Voltammetric peak potentials measured in DCM solution by SWV. [b]Calculated from $E_g^{CV} = E_{LUMO} - E_{HOMO}$.

HOMO and LUMO values were calculated using density functional theory. The HOMO values generally show a good match with experimental data (**Figure S7**) whereas the calculated LUMO values are consistently higher than the experimental values, but the trends in their relative values match those seen in the experimental data.

HOMO and LUMO orbital configurations can provide useful information on charge transfer interaction. Frontier Molecular Orbital (FMO) calculations **(Figure 5)** clearly show that in **DBP1**, **DBP3**, **DBP4**, and **DBP6** after excitation almost the same charge density distributions remain for HOMO and LUMO. However, in **DBP2** and **DBP5** there are well segregated HOMO and LUMO orbitals, which is indicative of intramolecular charge transfer between the heterocyclic moieties. This will be discussed below with regard to time-resolved fluorescence studies.

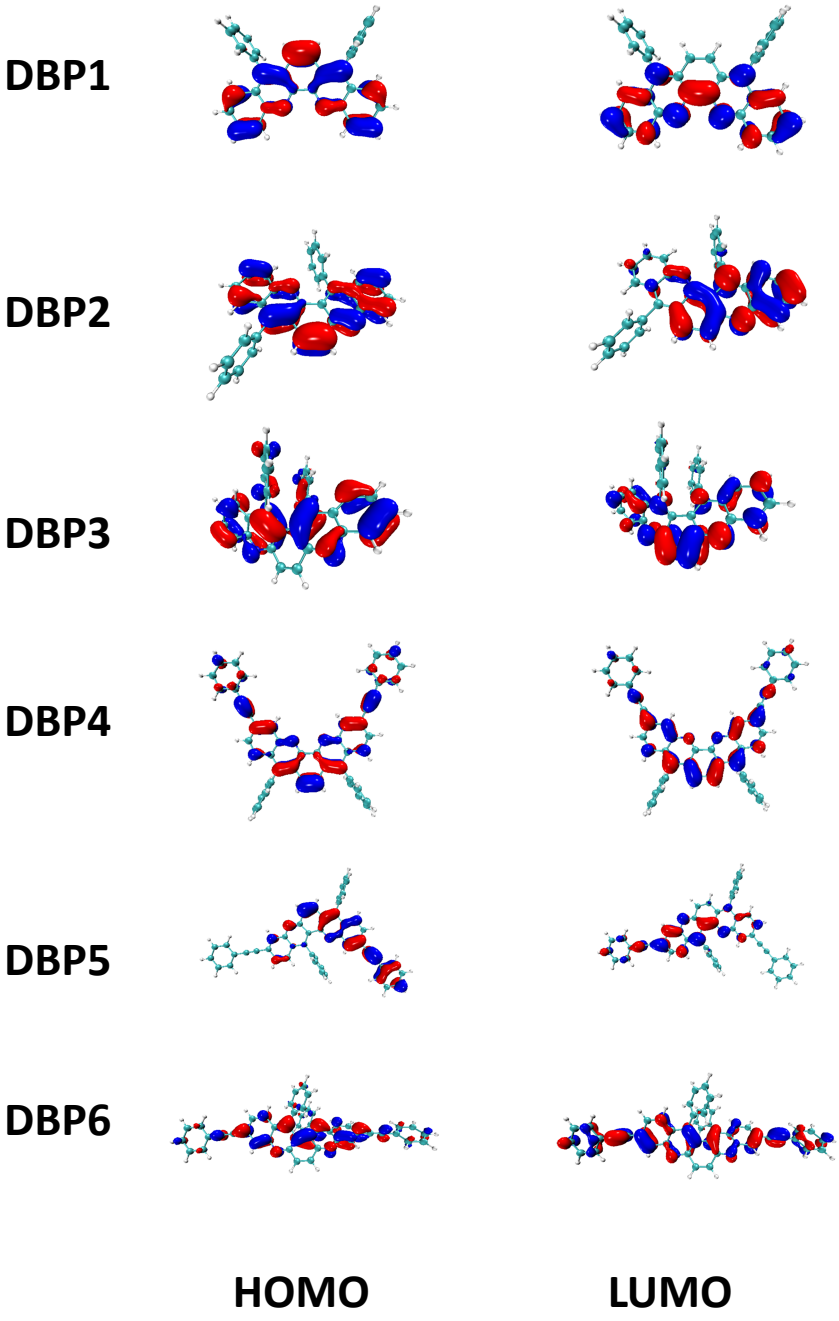

Figure 5. Electronic density distributions HOMO and LUMO energies for **DBP1-6**. Red and blue regions denote the positive and negative orbital phases, respectively. Green, blue and white balls represent carbon, nitrogen and hydrogen atoms, respectively. The calculations used B3LYP/6-311G(d,p) with PCM (DCM solvent).

Optical Properties

Photographs of chloroform solution of the dibenzophenanthroline isomers in daylight (top row) and under UV irradiation (bottom row) are shown in **Figure 6a (DBP1-3)** and **Figure 7a (DBP4-6)**. Both absorption and emission colours are dependent upon the specific structures. In daylight solutions of **DBP1**, **DBP2**, and **DBP3** are light yellow, colourless and light orange respectively while solutions of their bis(phenylethynyl) substituted analogues exhibit slightly deeper colour. Under UV irradiation the solution of **DBP2** displayed no visible fluorescence while solutions of **DBP1** and **DBP3** exhibited light blue and intense yellow fluorescence respectively. Bis(phenylethynyl) substitution resulted in a marked increase in fluorescence intensity for all compounds **DBP4-6** compared to their unsubstituted analogues.

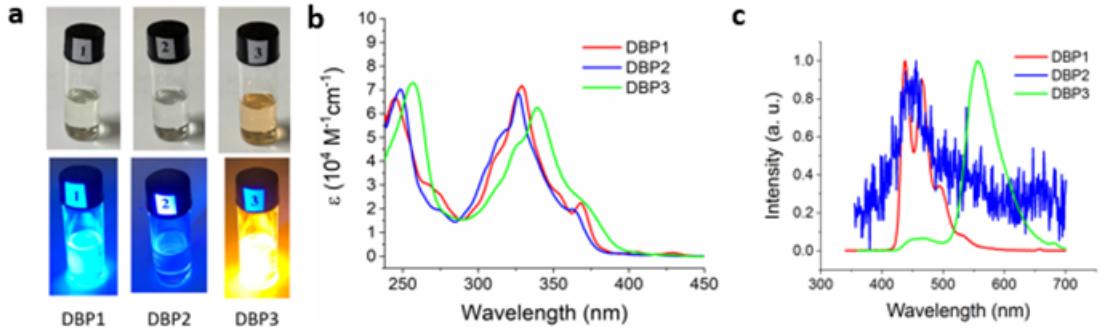

Figure 6. (a) Photographs of solutions of compounds **DBP1**, **DBP2**, and **DBP3** in $CHCl_3$ in ambient light (top row) and in dark with irradiation at 365 nm (bottom row). (b) UV−vis extinction coefficients (10^4 M^{-1} cm^{-1}) Vs absorption wavelength (nm) and (c) Normalized fluorescence spectra of **DBP1** (Red), **DBP2** (Blue) and **DBP3** (Green) in chloroform solution.

Electronic absorption and photoluminescence spectra of **DBP1**, **DBP2** and **DBP3** were measured in chloroform solution (**Figure 6b, 6c**). The first absorption bands of **DBP1**, **DBP2**

and **DBP3** have absorption maximum at 369, 364 and 373 nm respectively (**Table 2**). The absorption spectrum of **DBP1** and **DBP2** are blue shifted by 4 nm and 9 nm respectively compared to that of **DBP3** and hence the 0-0 transition of **DBP1** (3.15 eV) determined from the edge of absorption spectrum is smaller than that of **DBP2** (3.20 eV) while **DBP3** (2.99 eV) has the smallest 0-0 transition. The comparative optical HOMO-LUMO energy gaps suggest that **DBP3** has the most delocalised and **DBP2** the least delocalised π-electrons of the three isomers. The same trends were also observed in electrochemical studies (**Table 1**) of these isomers, but the optical bandgaps for **DBP1-3** were all 0.2-0.3 eV higher than their electrochemical bandgaps.

Table 2. Summary of Optical Properties of **DBP1**, **DBP2**, **DBP3, DBP4, DBP5 and DBP6**

Compound	$\lambda_{abs,\,max}$ [nm][a]	λ_{onset} [nm]	λ_{ex} [nm]	λ_{em} [nm][a]	ΔE_g^{opt} [eV][b]	Φ^a	Stokes shift [cm^{-1}]
DBP1	369, 329, 245	393	329	465, 438	3.15	0.076	4270
DBP2	364, 327, 248	387	327	451	3.20	0.001	5300
DBP3	373, 340, 257	414	340	556, 458	2.99	0.16	4980
DBP4	401, 381	478	400	452, 427	2.59	0.26	1520
DBP5	469, 441	540	467	476, 418	2.29	0.012	1270
DBP6	609, 478	690	368	661, 540	1.79	0.10	1400

[a]Measured in chloroform solution. [b]Estimated using the onset of the UV−vis spectrum in solution by $\Delta E_g^{opt} = 1240/\lambda_{onset}$.

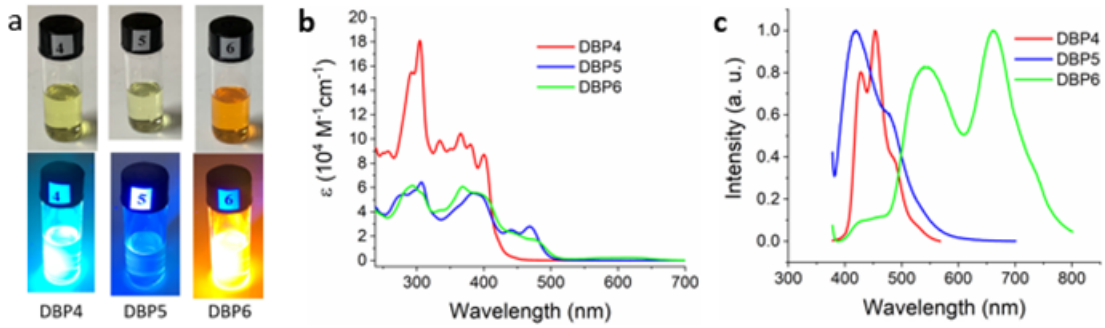

Figure 7. (a) Photographs of solutions of compounds **DBP4**, **DBP5** and **DBP6** in $CHCl_3$ in ambient light (top) and in dark with irradiation at 365 nm. (b) UV−vis extinction coefficients (10^4 M^{-1} cm^{-1}) Vs absorption wavelength (nm) and (c) Normalized PL spectra of **DBP4** (Red), **DBP5** (Blue) and **DBP6** (Green) in chloroform solution.

The absorption and emission spectra of **DBP4**, **DBP5** and **DBP6** were measured in chloroform solution and compared to their analogues **DBP1**, **DBP2** and **DBP3** (**Figure 7b, 7c**). The results are tabulated in **Table 2**. The absorption spectrum of **DBP4** exhibited vibronically split bands with a first absorption maxima at 401 nm indicating its more rigid molecular structure in comparison to **DBP5** and **DBP6**. The first absorption maximum of **DBP5** was at λ_{max}= 469 nm while **DBP6** exhibited a weaker absorption in the red part of the spectrum (540-700 nm) with the absorption maxima at 609 nm. LUMO-HOMO gaps estimated from the onset (λ_{onset} for **DBP4** and **DBP5** are 478 nm and 540 nm respectively) of UV-Vis absorption spectrum are calculated to be 2.59 eV for **DBP4** and 2.29 eV for **DBP5**. The dramatic redshift of absorption maximum of **DBP6** resulted in a contraction of its energy gap to 1.79 eV. There was a negligible difference between the electrochemical and optical energy gaps for the substituted compounds **DBP4-6**. The relative energy gaps suggest that amongst the three bis(phenylethynyl) substituted isomers, the π-electrons in **DBP4** are the least delocalized while those in **DBP6** are the most delocalized. The UV-vis absorption in solid state was investigated on thin films prepared by drop casting on quartz slide from chloroform solution (**Figure S2, S3**). The UV-vis spectra of **DBP1-3** in thin film, though

display similar nature, are a little red shifted (5-8 nm) in comparison to that in solution. In thin film, the first major peak of **DBP4** is red shifted by 43 nm, while that of **DBP5** is blue shifted by 15 nm and for **DBP6** the peak position remains same in comparison to that in solution.

As evidenced from the energy gap calculations in **Table 2**, introduction of phenyl acetylene groups to the dibenzophenanthrolines backbone has lowered the energy gap values of all three dibenzophenanthrolines isomers, indicating, as expected, that they contain an expanded π-system.

Emission spectra

Emission spectra of **DBP1**, **DBP2** and **DBP3** are displayed in **Figure 6c.** Both **DBP1** and **DBP3** exhibited two peaks at λem (465 nm, 438 nm) and at λem (556 nm, 458 nm) respectively with a shoulder while **DBP2** was almost non-emissive (inset). Emission spectra of **DBP3** demonstrated a large red shift with first emission maxima peaking at 556 nm and hence exhibited a much-enhanced quantum yield (=0.16) than that of **DBP1** (=0.076). **DBP2** was almost nonemissive as observed from its emission spectra (**Figure 6c**, inset) as well as quantum yield value (0.001).

Optical spectra of the compounds are displayed in **Figures 6** and **7** and the data are tabulated in **Table 2**. Stokes shifts of **DBP1-3** in chloroform are 4270, 5300 and 4980 cm^{-1} respectively. The Stokes shifts of **DBP2/3** are larger than that of **DBP1**. In **DBP2** the two nitrogen atoms and phenyl rings being on opposite sides, leads to delocalization of electron cloud as shown in **Figure 5** and an elevation of the π–π* state. In this case, we observe a larger Stokes shift. The emission spectrum of **DBP3** is of excimer origin. In **DBP3** two phenyl rings are in congested positions, which twist the backbone affecting the π stacking conjugation. It results in spontaneous aggregation that leads to red-shifted excimer-like emission bands. [27] Absorption and emission spectra of **DBP3** are independent of the

concentration, therefore in **DBP3** occurs intramolecular aggregation/complexation due to strongly twisted conformation of the acene ring. Two substituted phenyl rings are positioned close to each other which lead to steric repulsion between them causing a torsion in the molecules. Additionally, the large Stokes shift and long fluorescence lifetime (see below) are typical characteristics for excimer formation. [28-31] Therefore, the larger Stokes shift in **DBP3** is due to a complex configuration rearrangement of excited states. This comparison indicates how the N substitution in different position of dibenzophenanthrolines can modulate their optical properties.

Figure 7c displays the emission spectra of **DBP4**, **DBP5** and **DBP6**. Emission spectra of all the three bis(phenylethynyl)-substituted DBPs are redshifted in comparison to the unsubstituted heteroacene isomers. Emission spectra of **DBP4** and **DBP6** exhibited two well defined bands at λ_{em} (452 nm, 427 nm) and at λ_{em} (661 nm, 540 nm) respectively. Introduction of bis(phenylethynyl) substitution has resulted dramatic increase of its emission exhibiting one main band at 418 nm with a shoulder. The redshift in emission bands of bis(phenylethynyl) substituted isomers are attributed to their extended π-conjugation. Stokes shifts of **DBP4** and **5** in chloroform are 1520 and 1270 cm^{-1} respectively. Introduction of phenyl acetylene groups to the dibenzophenanthrolines backbone lowered the energy gap of all three dibenzophenanthrolines isomers, resulting in a small Stokes shift (compared with **DBP1** and **2**). It should be mentioned that for **DBP5** in chloroform the absorption band at 397 nm was used to calculate Stokes shift (compare with Figure S6e in SI). Similar to **DBP3**, in **DBP6** we have observed locally excited state (LE) and excimer emission. Two substituted phenyl rings are positioned close to each with steric repulsion between them, causing torsion in the molecules, which leads to an excimer kind of emission. Note that the Stokes shift in this case was calculated by using LE band. Interestingly, **DBP4** exhibited higher quantum yield than **DBP6** despite having a larger energy gap. The reason for this result is unclear.

The photoluminescence (PL) in solid state was investigated on thin films prepared by drop casting on glass slides from chloroform solution (**Figures S4, S5**). The main peak in the thin film emission spectra of **DBP1-3** exhibits a red shift of 20-30 nm in comparison to that in solution. The main peaks in the thin film emission spectra of bis(phenylethynyl)-substituted isomers **DBP4** and **DBP5** show red shifts of 59 nm and 56 nm respectively, while that of **DBP6** shows a blue shift by 74 nm in comparison to that in solution.

Time-resolved fluorescence spectroscopy

Steady-state absorption, fluorescence, and excitation spectra of **DBP**s dissolved in ethanol are shown in **Figure S6**. Note we use absorptance (1-T, where T is transmittance) as a linear scale of absorption instead of absorbance. Weak bands at 402, 425 nm for **DBP1** and 390, 413 nm for **DBP2** are assigned to $S_0 \rightarrow S_1$ transition with 1346 cm^{-1} and 1428 cm^{-1} vibronic progression, respectively. The latter shows a 12 nm blueshift compared with **DBP1**, indicating that the first excited state is higher due to the opposite location of N atoms and substituted phenyl rings. In addition, both show one pronounced peak at 325 nm, which can be assigned to S_2 state. In **DBP1,** fluorescence spectra display two maxima at 438 and 462 nm with a shoulder at 493 nm. However, emission of **DBP2** fully disappears due to an efficient quenching process, which will be discussed below. A similar trend in the absorption and fluorescence was observed for **DBP4** and **DBP5**. It should be mentioned that the structured S_1 bands at about 400 nm changes to a smooth absorption tail in the case of **DBP4** and **DBP5,** suggesting the existence of charge-transfer due to delocalization of the electron cloud as a result of bis(phenylethynyl) substitutions.[19] Moreover, going from **DBP1** to **DBP4** a redshift of 22 nm is observed in emission, indicating a progressive lowering of the $\pi-\pi*$ level, which moves away from the $n-\pi^*$ level.[20] Note that in dibenzophenathroline derivatives emission

arises from π–π* transitions.[19, 21] This will be discussed below with regard to time-resolved fluorescence studies.

Apart from these four **DBP**s, in the cases of **DBP3** and **DBP6** the broad absorption due to aggregation was observed ranging from 450 to 600 nm. We can exclude intermolecular aggregation in these two **DBPs** due to the independence of absorption/emission spectra from the concentration. Therefore, aggregation/complexation effect in **DBP3** and **DBP6** may occur inside the molecules themselves due to strongly twisted conformation of the acene ring. Two substituted phenyl rings are positioned close to each other which would lead to steric repulsion between them causing a torsion in the molecules. Moreover, **DBP3** and **DBP6,** compared with the previous compounds, show broader unstructured emission bands with much larger Stokes shifts.

In order to explore the origin of emission in **DBPs**, time-correlated single photon counting (TCSPC) technique was applied with λ_{exc} = 380 nm and the resulting fluorescence kinetics of **DBP1**, **DBP2**, **DBP4** and **DBP5** are presented in **Figure 8** and **Table 3**.

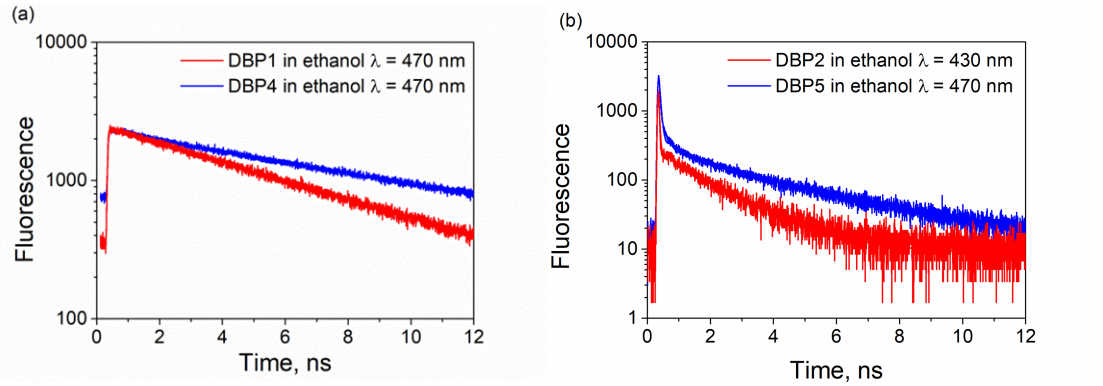

Figure 8. Decay kinetics of fluorescence of **DBP1, DBP4** (a) and **DBP2, DBP5** (b) in ethanol at different emission wavelengths.

Table 3. Lifetimes obtained from fit/deconvolution of fluorescence decay kinetics for **DBP1**, **DBP2**, **DBP4** and **DBP5** in ethanol at λ_{exc} = 380 nm (f = fixed).

Compound	$\lambda_{probe,}$ [nm]	τ_1, [ns]	A_1	τ_2, [ns]	A_2
DBP1	470			6.0	1
DBP2	430	0.03[f]	0.95	1.6	0.05
DBP4	470			8.1	1
DBP5	470	0.03[f]	0.95	2.7	0.05

The emission of **DBP1** and **DBP4** exhibits monoexponential decay with τ = 6.0 and 8.1 ns, respectively, originating from the locally excited singlet state S_1. Obviously, the extended π-conjugated bis(phenylethynyl) group (**DBP1** vs **DBP4**) results in longer (enhanced) emission. It demonstrates that the bis(phenylethynyl) substituted **DBP4** possesses larger π-π conjugation, which can lead to lower-lying π–π* state, thus enlarging π–π* and n–π* energy gap and prolonging the excited state lifetime due to proximity effect.[22] Surprisingly, when it turns to **DBP2** and **DBP5**, fluorescence decays biexponentially with a major component τ_1 << 30 ps (the time resolution of our setup) and a minor component τ_2 = 1.6 and 2.7 ns. These weak long components are responsible for the steady-state fluorescence with quantum yield ϕ < 0.1% and 1.2%, as discussed above. In these two compounds, steady-state emission almost fully disappears due to strong quenching.

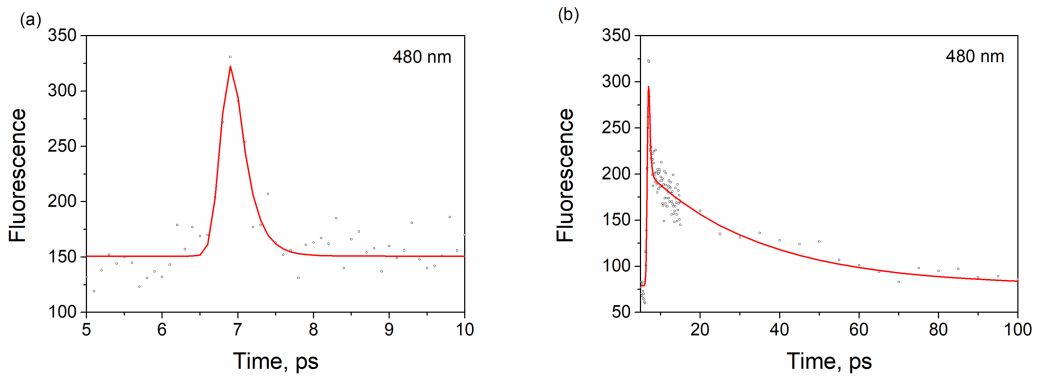

Figure 9. Fluorescence kinetics of **DBP2** (a) and **DBP5** (b) in ethanol measured by use of

fluorescence up-conversion technique, λ_{exc} = 400 nm.

Table 4. Lifetimes obtained from fit of fluorescence decay kinetics for **DBP2** and **DBP5** in ethanol (up-conversion data).

Compound	λ_{probe}, [nm]	τ_1, [ps]	A_1	τ_2, [ps]	A_2
DBP2	480	0.19	1		
DBP5	480	0.30	0.73	29	0.27

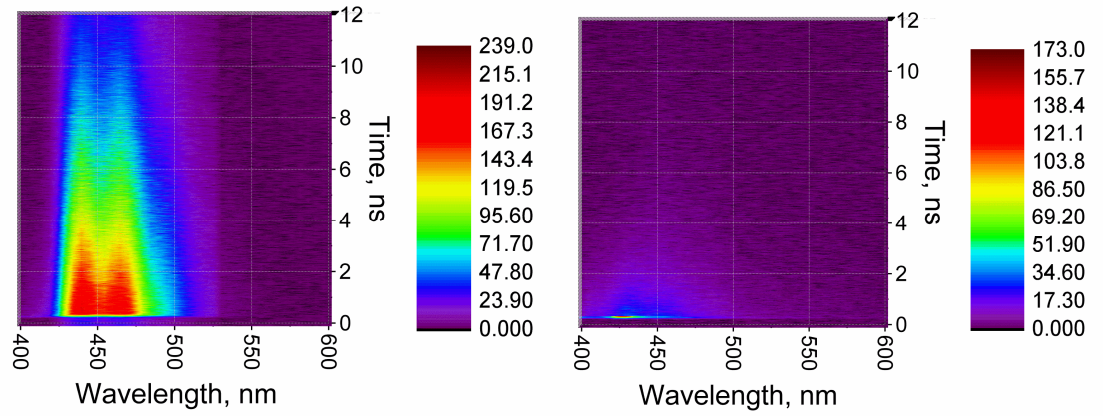

Figure 10. Fluorescence map of **DBP1** (a) and **DBP2** (b) in ethanol, λ_{exc} = 380 nm.

In order to resolve the ultrafast lifetime component of **DBP2** and **DBP5** emission, an up-conversion fluorescence technique was applied at λ_{exc} = 400 nm (**Figure 9**). At 480 nm, fluorescence decays with time constant τ = 0.19 ps in **DBP2** and biexponentially decays with τ_1 = 0.3 ps (73%) and τ_2 = 29 ps (27%) in **DBP5** (**Table 4**). We explain the ultrafast quenching process as being due to efficient charge transfer. In **DBP2**, the position of N and phenyl rings delocalizes the electron cloud, which leads to ultrafast intramolecular charge transfer within 190 fs. Similarly, introduction of phenyl acetylene groups to the dibenzophenanthroline backbone in **DBP5** results in lowering the singlet states, inducing the slower charge transfer within 29 ps. Accordingly the fluorescence quantum yield is increased more than an order of magnitude. The fluorescence of both **DBP2** and **DBP5** is strongly

quenched by intramolecular charge transfer, resulting in very weak emission. The time-resolved fluorescence results indicate that charge transfer in **DBP**2 is more efficient than **DBP5**. In turn, the fluorescence in **DBP2** is even weaker than of **DBP5**. Moreover, introduction of phenyl acetylene groups in **DBP5** enlarges the π-conjugation, leading to lower π–π* state and hence enhancing the fluorescence (compared with **DBP2**). Additionally, the structure of **DBP2** is asymmetrical [26], π-system of **DBP2** is less efficient (compared with **DBP1** and **DBP3** [23]), therefore the emission is weaker.

To conclude, in these four **DBP**s, extended π-conjugated structure determines a significant enhancement of fluorescence and respective increase of the fluorescence quantum yield.[19, 21a, 23] More clearly, fluorescence maps of **DBP1** and **DBP2** in ethanol show the same trend **(Figure 10)**. There exists stronger quenching of locally excited S_1 state in **DBP2** and **DBP5** compared with **DBP1** and **DBP4.**

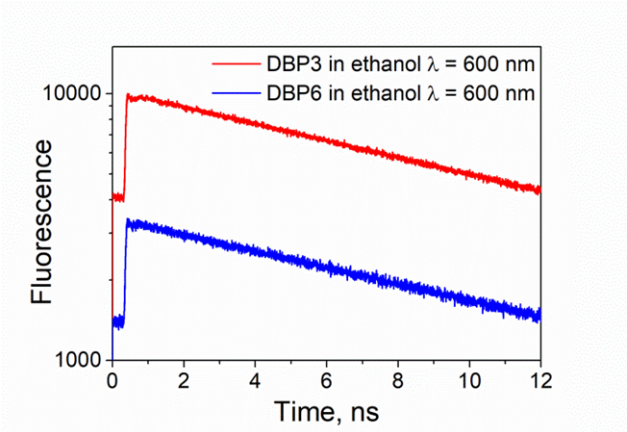

Figure 11. Decay kinetics of fluorescence of **DBP3** and **DBP6** in ethanol, λ_{probe} = 600 nm, λ_{exc} = 380 nm.

Table 5. Lifetimes obtained from fit/deconvolution of decay kinetics of fluorescence for **DBP3** and **DBP6** in ethanol.

Compound	λ_{probe}, [nm]	τ_1, [ns]	A_1
DBP3	600	13	1

DBP6	600	13	1

In **DBP3** and **DBP6,** absorption due to intramolecular aggregation was clearly observed in the steady-state spectra at 450-600 nm with the feature of broad and unstructured band. Accordingly, a strong structureless emission band was detected. These characteristic spectral features are indicative for excimer formation in the aggregated **DBP**s. Two substituted phenyl rings are positioned close to each other which would lead to steric repulsion between them causing a torsion in the molecules. It may lead to an excimer kind of emission. The fluorescence kinetics of **DBP3** and **DBP6** are presented in **Figure 11** and fitting results are shown in **Table 5**. The excimer emission of **DBP3** and **DBP6** at longer wavelengths 600-620 nm exhibits monoexponential decay with long time constant τ = 13 ns. Understandably, the fluorescence observed is much stronger than in the other four compounds (**Figure 10**). In these cases, excimer state with longer lifetime contributes mostly to the enhancement of fluorescence.

It should also be mentioned that **DBP3** and **DBP6** are highly sensitive to light. Therefore, a certain additional contribution of photoproducts to the fluorescence cannot be totally ruled out. DFT calculations on phenanthroline derivatives also show that 4,7-phenanthroline has lower ionization potential than 1,10- and 1,7-phenanthroline, i.e. 4,7-phenanthroline is less photostable.[24] In addition, **DBP3** and **DBP6** contain two phenyl rings in congested positions, which twist the backbone affecting the π-conjugation.[25]

Conclusion

In summary, we have developed efficient synthetic strategies for the synthesis of isomeric dibenzophenanthrolines and their bis(phenylethynyl) substituted analogues using Friedlander condensation and Sonogashira coupling as the key steps. The positions of the nitrogen atoms are found to profoundly affect their optoelectronic properties. Among the three

dibenzophenanthroline isomers prepared the 4,7-isomer **DBP3** possesses the smallest energy gap and exhibited most intense emission under UV light, but has lower photostability due to its higher HOMO energy. The PL enhancement of **DBP3** and its ethynyl substituted analogue **DBP6** is explained in terms of excimer formation, considering intramolecular aggregation phenomenon. Emission of the 1,7-phenthroline isomers **DBP2** and **DBP5** is strongly quenched by efficient charge transfer due to the position of the N substitution resulting in greater delocalization of the electron cloud. Moreover, introduction of bis(phenylethynyl) substituents lowered band gap values of all the three dibenzophenanthrolines isomers by expanding their π-system. It further enhanced the PL emission due to enlarging π–π∗ and n–π∗ energy gap and prolonging the excited state lifetime. We believe this synthetic strategy will be useful for the preparation of other heteroacenes and that dibenzophenthrolines have potential as active materials in devices such as OLEDs or OPVs.

Experimental Section

Synthesis of 5,8-diphenyl-6,7-dihydrodibenzo[b,j][1,10]phenanthroline (2)

Conc. HCl (2.64 mL, 31.7 mmol, 2.5 equiv) was added to a mixture of 2-aminobenzophenone (5.0 g, 25.3 mmol, 2 equiv) and 1,2-cyclohexanedione (1.4 g, 12.6 mmol, 1.0 equiv) in ethanol taken in a Schlenk flask under N_2 atmosphere at room temperature. The flask was capped and the reaction mixture was stirred at 80 °C for 24 hours. The reaction mixture was cooled and ethanol was evaporated under reduced pressure. The residue was diluted with 10% aqueous Na_2CO_3 (50 mL) and extracted with CH_2Cl_2 (2 x 100 mL). The CH_2Cl_2 extracts were combined, dried over $MgSO_4$, filtered, and evaporated. The residue was purified by column chromatography on silica gel (EtOAc/CH_2Cl_2 3:7) to afford compound **2** (4.6 g, 84%) as a yellow solid. ^{1}H NMR (400 MHz, $CDCl_3$) δ 8.53 (s, 1H), 8.51 (s, 1H), 7.73–7.67 (m, 2H), 7.54–7.41 (m, 10H), 7.34–7.28 (m, 4H), 2.83 (s, 4H); ^{13}C NMR (100 MHz, $CDCl_3$) δ 152.5, 147.8, 145.9, 136.5, 131.2, 130.1, 129.5, 128.5 (2), 128.0, 127.6, 127.0, 125.8, 26.2.

Synthesis of 5,8-diphenyldibenzo[b,j][1,10]phenanthroline (DBP1)

To a solution of compound **2** (2.0 g, 4.6 mmol, 1.0 equiv) in 1,2-dichloroethane (50ml) was added in N-Bromosuccinimide (0.98 g, 5.5 mmol, 1.2 equiv) followed by benzoyl peroxide (0.17g, 0.69 mmol, 0.15 equiv) under a nitrogen atmosphere. The reaction mixture was heated at 85 °C for 20 hours. It was diluted with 10% aqueous Na_2CO_3 solution (20 mL) and extracted with CH_2Cl_2 (2 x 50 mL). The CH_2Cl_2 extracts were combined, dried over $MgSO_4$, filtered, and evaporated. The residue was purified by column chromatography on silica gel (EtOAc/CH_2Cl_2 4:6) to afford **DBP1** (1.1 g, 55%) as a yellow solid. Mp: > 400 ºC. ^{1}H NMR (400 MHz, $CDCl_3$) δ 8.77 (d, J = 8.0 Hz, 2H), 7.91–7.83 (m, 2H), 7.75 (d, J = 8.0 Hz, 2H), 7.62–7.53 (m, 8H), 7.48–7.44 (m, 4H), 7.36 (s, 2H); ^{13}C NMR (100 MHz, $CDCl_3$) δ 147.8, 147.6, 146.5, 135.9, 131.6, 130.4, 129.4, 128.5, 128.3, 127.0, 126.7, 126.3, 124.9, 124.5. HRMS (ESI) m/z calcd for $C_{32}H_{21}N_2$ $[M+H]^+$ = 433.1699; found 433.1700.

Synthesis of 8,14-diphenyl-6,7-dihydrodibenzo[b,j][1,7]phenanthroline (3)

Conc. HCl (2.64 mL, 31.7 mmol, 2.5 equiv) was added to a mixture of 2-aminobenzophenone (5.0 g, 25.3 mmol, 2 equiv) and 1,3-cyclohexanedione (1.4 g, 12.6 mmol, 1.0 equiv) in ethanol taken in a Schlenk flask under N_2 atmosphere at room temperature. The flask was capped and the reaction mixture was stirred at 80 °C for 60 hours. The reaction mixture was cooled and ethanol was evaporated under reduced pressure. The residue was diluted with 10% aqueous Na_2CO_3 (50 mL) and extracted with CH_2Cl_2 (2 x 100 mL). The CH_2Cl_2 extracts were combined, dried over $MgSO_4$, filtered, and evaporated. The residue was purified by column chromatography on silica gel (EtOAc/CH_2Cl_2/Hexane 2:1:7) to afford compound **3** (2.2 g, 40%) as a yellow solid. ^{1}H NMR (400 MHz, $CDCl_3$) δ 8.12–8.07 (m, 1H), 7.72–7.66 (m, 2H), 7.55–7.23 (m, 15H), 3.33–3.24 (m, 2H), 3.03–2.93 (m, 2H); ^{13}C NMR (100 MHz, $CDCl_3$) δ 160.8, 152.2, 147.8, 147.4, 146.2, 144.5, 139.1, 136.5, 129.7,

129.6, 129.5(2), 128.5(2), 128.3, 128.1, 127.9, 127.6, 127.5, 126.6, 126.3, 126.1, 126.0, 125.8, 125.6, 33.9, 26.0.

Synthesis of 8,14-diphenyldibenzo[b,j][1,7]phenanthroline (DBP2)

To the suspension of compound **3** (2.96 g, 6.82 mmol, 1.0 equiv) in xylene (20 mL) taken in a round bottom flask was added 2,3-dichloro-5,6-dicyanobenzoquinone (DDQ) (1.5 g, 6.82 mmol, 1.0 equiv). Nitrogen was bubbled through the mixture for 5 min before the flask was capped and heated at 110 °C for 3 hours. The reaction mixture was cooled to room temperature, diluted with water (50 mL) and extracted with CH_2Cl_2 (2 x 100 mL). The CH_2Cl_2 extracts were combined, dried over $MgSO_4$, filtered and concentrated. The dark brown residue was purified by column chromatography on silica gel (EtOAc/CH_2Cl_2/Hexane 1:1:8) to afford **DBP2** (1.7 g, 58%) as a light grey solid. Mp: 280 °C. ^{1}H NMR (400 MHz, $CDCl_3$) δ 8.32 (d, J = 8.0 Hz, 1H), 7.90–7.79 (m, 3H), 7.72–7.50 (m, 10H), 7.44–7.37 (m, 5H), 7.27 (d, J = 8.0 Hz, 1H); ^{13}C NMR (100 MHz, $CDCl_3$) δ 151.4, 149.1, 148.3, 147.8, 145.5, 145.4, 141.7, 135.9, 130.4, 130.2(2), 129.8, 129.5, 129.2, 129.0, 128.9, 128.5, 128.3, 128.0, 127.8, 127.7, 126.5, 126.4, 126.1, 126.0, 125.1, 123.0, 122.5. HRMS (ESI) m/z calcd for $C_{32}H_{21}N_2$ $[M+H]^+$ = 433.1699; found 433.1700.

Synthesis of 13,14-diphenyl-6,7-dihydrodibenzo[b,j][4,7]phenanthroline (4)

Conc. HCl (2.64 mL, 31.7 mmol, 2.5 equiv) was added to a mixture of 2-aminobenzophenone (5.0 g, 25.3 mmol, 2 equiv) and 1,4-cyclohexanedione (1.4 g, 12.6 mmol, 1.0 equiv) in ethanol taken in a Schlenk flask under N_2 atmosphere at room temperature. The flask was capped and the reaction mixture was stirred at 80 °C for 22 hours. The reaction mixture was cooled and ethanol was evaporated under reduced pressure. The residue was diluted with 10% aqueous Na_2CO_3 (50 mL) and extracted with CH_2Cl_2 (2 x 100 mL). The CH_2Cl_2 extracts were combined, dried over $MgSO_4$, filtered, and evaporated. The residue was purified by column chromatography on silica gel (EtOAc/CH_2Cl_2 3:7) to afford

compound 3 (4.7 g, 90%) as a yellow solid. ^{1}H NMR (400 MHz, CDCl^{3}) δ 8.08 (d, J = 8.0 Hz, 2H), 7.72–7.61 (m, 4H), 7.34–7.26 (m, 2H), 7.22–7.16 (m, 2H), 7.06 (brs, 4H), 6.48 (brs, 4H), 3.50–3.28 (m, 4H); ^{13}C NMR (100 MHz, $CDCl_3$) δ 162.4, 147.0, 146.2, 135.4, 131.3, 129.3, 128.7,128.1, 127.4, 126.0, 125.8, 125.7, 124.9, 34.9.

Synthesis of 13,14-diphenyldibenzo[b,j][4,7]phenanthroline (DBP3)

To the suspension of compound **4** (1.19 g, 2.74 mmol, 1.0 equiv) in xylene (20 mL) taken in a round bottom flask was added 2,3-dichloro-5,6-dicyanobenzoquinone (DDQ) (0.62 g, 2.74 mmol, 1.0 equiv). Nitrogen was bubbled through the mixture for 5 min before the flask was capped and heated at 110 °C for 3 hours. The reaction mixture was cooled to room temperature, diluted with water (50 mL) and extracted with CH_2Cl_2 (2 x 100 mL). The CH_2Cl_2 extracts were combined, dried over $MgSO_4$, filtered and concentrated. The dark brown residue was purified by column chromatography on silica gel (EtOAc/CH_2Cl_2 1:1) to afford compound **DBP3** (540 mg, 46%) as a purple solid. Mp: 260 ºC. ^{1}H NMR (400 MHz, $CDCl_3$) δ 8.23 (d, J = 8.0 Hz, 2H), 7.92 (s, 2H), 7.81 (d, J = 8.0 Hz, 2H), 7.75–7.69 (m, 2H), 7.39–7.33 (m, 2H), 7.25–7.19 (m, 2H), 7.18–6.95 (brs, 4H), 6.51 (d, J = 8.0 Hz, 4H); ^{13}C NMR (100 MHz, $CDCl_3$) δ 151.1, 147.8, 147.2, 136.5, 133.5, 131.4, 129.7, 129.2, 128.5, 127.4, 126.4, 125.9, 124.1, 121.9. HRMS (ESI) m/z calcd for $C_{32}H_{21}N_2$ $[M+H]^+$ = 433.1699; found 433.1701.

2,11-dibromo-5,8-diphenyl-6,7-dihydrodibenzo[b,j][1,10]phenanthroline (6)

Conc HCl (1.68 mL, 20.17 mmol) was added to a mixture of (2-amino-4-bromophenyl)(phenyl)methanone (4.46 g, 16.1 mmol) and cyclohexane-1,2-dione (906 mg, 8.07 mmol) in ethanol (50 mL) taken in a Schlenk flask under N_2 atmosphere at room temperature. The flask was capped and the reaction mixture was stirred at 80 ºC for 20 h. The reaction mixture was cooled and the ethanol was evaporated under reduced pressure. The residue was diluted with 5% aqueous Na_2CO_3 (50 mL) and extracted with DCM (2 x 100

mL). The organic extracts were combined, dried ($MgSO_4$), filtered and concentrated. The residue was purified by column chromatography on silica gel (ethyl acetate/DCM/hexane 10:5:85) to afford **6** as a yellow solid (3.92 g, 82%). ^{1}H NMR (400 MHz, $CDCl_3$) δ 8.71 (d, J = 4.0 Hz, 2H), 7.57-7.48 (m, 8H), 7.36 (d, J = 8.0 Hz, 2H), 7.31-7.27 (m, 4H), 2.82 (s, 4H); ^{13}C NMR (100 MHz, $CDCl_3$) δ 153.1, 148.4, 146.3, 135.8, 133.2, 130.6, 129.3, 128.7, 128.3, 127.3, 126.4, 123.0, 26.0.

2,11-dibromo-5,8-diphenyldibenzo[b,j][1,10]phenanthroline (7)

To a solution of 2,11-dibromo-5,8-diphenyl-6,7-dihydrodibenzo[b,j][1,10]phenanthroline (500 mg, 0.84 mmol) in 1,2-dichloroethane (20 mL) was added N-bromosuccinimide (180 mg, 1.01 mmol) followed by benzoyl peroxide (31 mg, 0.12 mmol) under a nitrogen atmosphere. The reaction mixture was heated at 80 ^{o}C for 24 h. The reaction mixture was cooled to room temperature, diluted with 5% aqueous Na_2CO_3 (20 mL) and extracted with DCM (2 x 50 mL). The organic extracts were combined, dried ($MgSO_4$), filtered and concentrated. The residue was purified by column chromatography on silica gel (ethyl acetate/DCM 10:90) to afford **7** as a yellow solid (307 mg, 62%). ^{1}H NMR (400 MHz, $CDCl_3$) δ 8.98 (s, 2H), 7.65-7.57 (m, 10H), 7.47-7.41 (m, 4H), 7.37 (s, 2H).

5,8-diphenyl-2,11-bis(phenylethynyl)dibenzo[b,j][1,10]phenanthroline (DBP4)

N_2 (g) was bubbled through a mixture of 2,11-dibromo-5,8-diphenyldibenzo[b,j][1,10]phenanthroline (90 mg, 0.15 mmol) $Pd(PPh_3)_2Cl_2$ (3.2 mg, 0.004 mmol), CuI (1.0 mg, 0.005 mmol), Et_3N (0.34 mL, 2.43 mmol) and anhydrous DMF (3 mL) taken in a Schlenk flask at room temperature for 5 min before the addition of phenyl acetylene (0.05 mL, 0.45 mmol). The flask was capped and the reaction mixture was stirred at 110 ^{o}C overnight. The reaction mixture was cooled to room temperature, filtered through celite and washed with Ethyl acetate (15 mL). The organic layer was washed with water,

dried ($MgSO_4$), filtered and concentrated. The residue was purified by column chromatography on silica gel (ethyl acetate/DCM/hexane 10:15:75) to afford **DBP4** as a yellow solid (45 mg, 48%). Mp: > 400 ^oC. ^1H NMR (400 MHz, $CDCl_3$) δ 8.96 (s, 2H), 7.73-7.58 (m, 14H), 7.49-7.46 (m, 4H), 7.44-7.40 (m, 6H), 7.37 (s, 2H); ^{13}C NMR (100 MHz, $CDCl_3$) δ 148.1, 147.4, 146.4, 135.5, 134.4, 131.9, 130.4, 129.6, 128.6 (2), 128.5, 128.4, 126.4, 126.3, 125.3, 124.7, 124.6, 123.0, 92.2, 89.4; HRMS (ESI) m/z calcd for $C_{48}H_{29}N_2$ $[M+H]^+$ = 633.2325; found 633.2323.

3,11-dibromo-8,14-diphenyl-6,7-dihydrodibenzo[b,j][1,7]phenanthroline (8)

Conc HCl (0.45 mL, 5.42 mmol) was added to a mixture of (2-amino-4-bromophenyl)(phenyl)methanone (1.2 g, 4.3 mmol) and cyclohexane-1,3-dione (243 mg, 2.17 mmol) in ethanol (20 mL) taken in a Schlenk flask under N_2 atmosphere at room temperature. The flask was capped and the reaction mixture was stirred at 80 ^oC for 48 h. The reaction mixture was cooled and the ethanol was evaporated under reduced pressure. The residue was diluted with 5% aqueous Na_2CO_3 (50 mL) and extracted with DCM (2 x 100 mL). The organic extracts were combined, dried ($MgSO_4$), filtered and concentrated. The residue was purified by column chromatography on silica gel (ethyl acetate/DCM/hexane 10:5:85) to afford **8** as a yellow solid (361 mg, 28%). ^1H NMR (400 MHz, $CDCl_3$) δ 8.28 (d, J = 4.0 Hz, 1H), 7.59-7.48 (m, 8H), 7.42-7.29 (m, 6H), 7.23 (d, J = 8.0 Hz, 1H), 3.30-3.23 (m, 2H), 3.00-2.93 (m, 2H); ^{13}C NMR (100 MHz, $CDCl_3$) δ 161.8, 152.9, 148.2, 148.1, 146.9, 144.9, 138.3, 135.9, 131.5, 129.6 (2), 129.4 (2), 128.7, 128.3, 127.9,131.3, 130.9, 130.7, 129.9, 129.0, 127.1, 126.0, 124.9, 124.4, 122.4, 33.7, 25.9.

3,11-dibromo-8,14-diphenyldibenzo[b,j][1,7]phenanthroline (9)

To a solution of 3,11-dibromo-8,14-diphenyl-6,7-dihydrodibenzo[b,j][1,7]phenanthroline (361 mg, 0.61 mmol) in xylene (15 mL) was added DDQ (138 mg, 0.61 mmol) under a

nitrogen atmosphere. The reaction mixture was heated at 110 ºC for 3 h. The reaction mixture was cooled to room temperature, diluted with 10% aqueous NaOH (20 mL) and extracted with DCM (2 x 30 mL). The organic extracts were combined, dried ($MgSO_4$), filtered and concentrated. The residue was purified by column chromatography on silica gel (ethyl acetate/DCM 5:95) to afford **9** as a yellow solid (330 mg, 92%). ^{1}H NMR (400 MHz, $CDCl_3$) δ 8.49 (d, J = 4.0 Hz, 1H), 7.86-7.55 (m, 10H), 7.49-7.32 (m, 7H); ^{13}C NMR (100 MHz, $CDCl_3$) δ 152.1, 149.5, 148.8, 148.4, 145.9, 145.8, 140.8, 135.2, 132.1, 131.1, 130.2, 130.0, 129.9, 129.8, 129.6, 129.2, 128.7, 128.6(2), 128.2, 127.6, 126.8, 126.3, 125.1, 123.8, 123.7, 123.1, 122.4.

8,14-diphenyl-3,11-bis(phenylethynyl)dibenzo[b,j][1,7]phenanthroline (DBP5)

N_2 (g) was bubbled through a mixture of 3,11-dibromo-8,14-diphenyldibenzo[b,j][1,7]phenanthroline (330 mg, 0.56 mmol) $Pd(PPh_3)_2Cl_2$ (12 mg, 0.016 mmol), CuI (4.0 mg, 0.02 mmol), Et_3N (1.2 mL, 8.9 mmol) and anhydrous DMF (8 mL) taken in a Schlenk flask at room temperature for 5 min before the addition of phenyl acetylene (0.18 mL, 1.67 mmol). The flask was capped and the reaction mixture was stirred at 110 ºC overnight. The reaction mixture was cooled to room temperature, filtered through celite and washed with Ethyl acetate (15 mL). The organic layer was washed with water, dried (MgSO4), filtered and concentrated. The residue was purified by column chromatography on silica gel (ethyl acetate/DCM/hexane 15:20:65) to afford **DBP5** as a yellow solid (148 mg, 42%). Mp: 301 ºC. ^{1}H NMR (400 MHz, $CDCl_3$) δ 8.49 (d, J = 4.0 Hz, 1H), 7.88 (d, J = 12.0 Hz, 1H), 7.80-7.52 (m, 14H), 7.50-7.37 (m, 12H); ^{13}C NMR (100 MHz, $CDCl_3$) δ 152.0, 149.0, 148.4, 148.0, 145.3, 145.1, 141.2, 135.6, 133.2, 132.1, 131.8, 131.7, 130.4, 130.1, 129.6, 129.1, 128.7, 128.6(2), 128.5(2), 128.4(2), 128.2, 127.8, 127.3, 126.8,

126.2, 125.3, 124.8, 124.2, 123.4, 123.0, 122.9, 122.7, 92.3, 91.7, 89.4, 89.3; HRMS (ESI) m/z calcd for $C_{48}H_{29}N_2$ $[M+H]^+$ = 633.2325; found 633.2329.

3,10-dibromo-13,14-diphenyl-6,7-dihydrodibenzo[b,j][4,7]phenanthroline (10)

Conc HCl (0.94 mL, 11.3 mmol) was added to a mixture of (2-amino-4-bromophenyl)(phenyl)methanone (2.5 g, 9.05 mmol) and cyclohexane-1,4-dione (507 mg, 4.52 mmol) in ethanol (30 mL) taken in a Schlenk flask under N_2 atmosphere at room temperature. The flask was capped and the reaction mixture was stirred at 80 ^oC for 20 h. The reaction mixture was cooled and the ethanol was evaporated under reduced pressure. The residue was diluted with 5% aqueous Na_2CO_3 (50 mL) and extracted with DCM (2 x 100 mL). The organic extracts were combined, dried ($MgSO_4$), filtered and concentrated. The residue was purified by column chromatography on silica gel (ethyl acetate/DCM/hexane 20:40:40) to afford **10** as a grey solid (2.45 g, 91%).^{1}H NMR (400 MHz, $CDCl_3$) δ 8.25 (d, J = 4.0 Hz, 2H), 7.56 (s, 1H), 7.53 (s, 1H), 7.42-7.36 (m, 2H), 7.23 (t, J = 8.0 Hz, 2H), 7.09 (brs, 4H), 6.43 (brs, 4H), 3.46-3.29 (m, 4H); ^{13}C NMR (100 MHz, $CDCl_3$) δ 163.4, 147.8, 146.3, 134.9, 131.1, 129.2, 128.4, 127.8, 127.5, 124.9, 124.6, 123.8, 34.8.

3,10-dibromo-13,14-diphenyldibenzo[b,j][4,7]phenanthroline 5-oxide (11)

A solution of 3,10-dibromo-13,14-diphenyl-6,7-dihydrodibenzo[b,j][4,7]phenanthroline (1.40 g, 2.36 mmol) in $CHCl_3$ (70 mL) was cooled to 0 ^oC with an ice-water cooling bath. To this solution was added *m*-chloroperbenzoic acid (408 mg, 2.36 mmol) portionwise. The resulting yellow suspension was warmed up to room temperature over 1 h and stirred at room temperature for 7 h. The reaction mixture was poured into ice-water and aqueous NaOH (4M) was added dropwise to adjust pH to 12. The resulting solution was extracted with DCM (2 x 100 mL). The organic extracts were combined, dried ($MgSO_4$), filtered and concentrated. The residue was purified by column chromatography on silica gel (ethyl acetate/DCM 1:1) to afford **11** as a yellow solid (515 mg, 36%).^{1}H NMR (400 MHz, $CDCl_3$) δ 9.11 (d, J = 4.0 Hz,

1H), 8.27 (d, J = 4.0 Hz, 1H), 7.63-7.50 (m, 3H), 7.44-7.38 (m, 1H), 7.26-7.22 (m, 2H), 7.10 (brs, 4H), 6.42 (brs, 4H), 4.48-4.38 (m, 1H), 3.50-3.40 (m, 1H), 3.34-3.22 (m, 1H), 3.03-2.90 (m, 1H).

3,10-dibromo-13,14-diphenyldibenzo[b,j][4,7]phenanthroline (12)

To a solution of 3,10-dibromo-13,14-diphenyldibenzo[b,j][4,7]phenanthroline 5-oxide 3 (500 mg, 0.82 mmol) in DCM (10 mL) at 0 ºC was added trifluoroacetic acid anhydride (0.17 mL, 0.23 mmol) dropwise over a period of 5 min. The reaction mixture was stirred 30 min at 0 ºC followed by 4 h at room temperature. The reaction was quenched by the addition of ice-water (10 g) and the pH was adjusted to 12 by dropwise addition of 2M aqueous NaOH solution. The resulting mixture was stirred at room temperature for 16 hours. The reaction mixture was diluted with water (20 mL) and extracted with DCM (2 x 30 mL). The organic extracts were combined, dried ($MgSO_4$), filtered and concentrated. The residue was purified by column chromatography on silica gel (ethyl acetate/DCM 1:4) to afford **12** as a yellow solid (395 mg, 81%). ^{1}H NMR (400 MHz, $CDCl_3$) δ 8.41 (d, J = 4.0 Hz, 2H), 7.91 (s, 2H), 7.69 (s, 1H), 7.66 (s, 1H), 7.47-7.42 (m, 2H), 7.31-7.25 (m, 2H), 7.11 (brs, 4H), 6.48 (d, J = 8.0 Hz, 4H); ^{13}C NMR (100 MHz, $CDCl_3$) δ 151.8, 148.4, 147.4, 136.1, 133.9, 131.4, 131.3, 130.0, 128.8, 127.8, 127.5, 124.4, 122.9, 122.0.

13,14-diphenyl-3,10-bis(phenylethynyl)dibenzo[b,j][4,7]phenanthroline (DBP6)

N_2 (g) was bubbled through a mixture of 3,10-dibromo-13,14-diphenyldibenzo[b,j][4,7]phenanthroline (100 mg, 0.17 mmol) $Pd(PPh_3)_2Cl_2$ (3.6 mg, 0.005 mmol), CuI (1.2 mg, 0.006 mmol), Et_3N (0.38 mL, 2.7 mmol) and anhydrous DMF (4 mL) taken in a Schlenk flask at room temperature for 5 min before the addition of phenyl acetylene (0.056 mL, 0.51 mmol). The flask was capped and the reaction mixture was stirred at 110 ºC overnight. The reaction mixture was cooled to room temperature, filtered through celite and washed with Ethyl acetate (15 mL). The organic layer was washed with water,

dried ($MgSO_4$), filtered and concentrated. The residue was purified by column chromatography on silica gel (ethyl acetate/DCM/hexane 15:10:75) to afford **DBP6** as a yellow solid (52 mg, 48%). Mp: 311 °C. ^{1}H NMR (400 MHz, $CDCl_3$) δ 8.41 (s, 2H), 7.94 (s, 2H), 7.81 (s, 1H), 7.78 (s, 1H), 7.66-7.56 (m, 4H), 7.50-7.24 (m, 10H), 7.14 (brs, 4H), 6.53 (d, J = 8.0 Hz, 4H); ^{13}C NMR (100 MHz, $CDCl_3$) δ 151.8, 147.6, 147.0, 136.3, 133.8, 132.3, 131.8, 131.4, 129.0, 128.7, 128.4, 127.7, 126.1, 124.8, 123.7, 122.9, 122.2, 92.3, 89.0; HRMS (ESI) m/z calcd for $C_{48}H_{29}N_2$ $[M+H]^+$ = 633.2325; found 633.2324.

Acknowledgements

We thank Ms Chua Wen Ying for assistance in the synthesis, Dr. Xiaoxuan Chen and Assoc. Prof. Sun Handong from Division of Physics and Applied Physics, SPMS, NTU for assistance in measuring the quantum yields. We acknowledge funding from the Singapore Ministry of Education through the Academic Research Fund (RG117/15 and MOE2019-T2-1-085).

Conflicts of Interest

We have no conflicts of interest to declare.

Keywords: cyclic voltammetry, Friedländer reaction, heteroacenes, organic semiconductor, photoluminescence.

References

[1] a) M. Yamada, I. Ikemoto, H. Kuroda, *Bull. Chem. Soc. Jpn.* **1988**, *61*, 1057-1062; b) J.-M. Aubry, C. Pierlot, J. Rigaudy, R. Schmidt, *Acc.Chem. Res.* **2003**, *36*, 668-675.

[2] a) O. D. Jurchescu, J. Baas, T. T. M. Palstra, *Appl. Phys. Lett.* **2004**, *84*, 3061-3063; b) J. E. Anthony, *Angew. Chem. Int. Ed.* **2008**, *47*, 452-483.

[3] a) X.-Y. Wang, F.-D. Zhuang, R.-B. Wang, X.-C. Wang, X.-Y. Cao, J.-Y. Wang, J. Pei, *J. Am Chem. Soc.* **2014**, *136*, 3764-3767; b) X.-Y. Wang, J.-Y. Wang, J. Pei, *Chem. –Eur. J.* **2015**, *21*, 3528-3539; c) P. G. Campbell, A. J. V. Marwitz, S.-Y. Liu, *Angew. Chem. Int. Ed.* **2012**, *51*, 6074-6092; d) J. Chen, J. W. Kampf, A. J. Ashe, *Organometallics* **2008**, *27*, 3639-3641; e) G. Long, X. Yang, W. Chen, M. Zhang, Y. Zhao, Y. Chen, Q. Zhang, *Phys. Chem. Chem. Phys.* **2016**, *18*, 3173-3178; f) L. Ren, C. Liu, Z. Wang, X. Zhu, *J. Mater. Chem. C* **2016**, *4*, 5202-5206; g) T. Zheng, Z. Cai, R. Ho-Wu, S. H. Yau, V. Shaparov, T. Goodson, L. Yu, *J. Am Chem. Soc.* **2016**,

138, 868-875; h) U. H. F. Bunz, *Chem. –Eur. J.* **2009**, *15*, 6780-6789; i) U. H. F. Bunz, *Pure Appl. Chem.* **2010**, *82*, 953-968; j) U. H. F. Bunz, J. U. Engelhart, B. D. Lindner, M. Schaffroth, *Angew. Chem. Int. Ed.* **2013**, *52*, 3810-3821; k) J. U. Engelhart, O. Tverskoy, U. H. F. Bunz, *J. Am Chem. Soc.* **2014**, *136*, 15166-15169; l) Q. Miao, *Synlett* **2012**, *2012*, 326-336; m) Q. Miao, *Adv. Mater.* **2014**, *26*, 5541-5549; n) G. J. Richards, J. P. Hill, T. Mori, K. Ariga, *Org. Biomol. Chem.* **2011**, *9*, 5005-5017.

[4] D. Xia, X. Guo, L. Chen, M. Baumgarten, A. Keerthi, K. Müllen, *Angew. Chem. Int. Ed.* **2016**, *55*, 941-944.

[5] a) J. Chen, K. Yang, X. Zhou, X. Guo, *Chem. –Asian J.* **2018**, *13*, 2587-2600; b) S. Hahn, F. L. Geyer, S. Koser, O. Tverskoy, F. Rominger, U. H. F. Bunz, *J. Org. Chem.* **2016**, *81*, 8485-8494; c) M. Tasior, D. T. Gryko, *J. Org. Chem.* **2016**, *81*, 6580-6586; d) Y. C. Teo, Z. Jin, Y. Xia, *Org. Lett.* **2018**, *20*, 3300-3304; e) F. Ding, D. Xia, W. Sun, W. Chen, Y. Yang, K. Lin, F. Zhang, X. Guo, *Chem. –Eur. J.* **2019**, *25*, 15106-15111.

[6] a) S. Hahn, S. Koser, M. Hodecker, O. Tverskoy, F. Rominger, A. Dreuw, U. H. F. Bunz, *Chem. –Eur. J.* **2017**, *23*, 8148-8151; b) S. Hahn, P. Biegger, M. Bender, F. Rominger, U. H. F. Bunz, *Chem. –Eur. J.* **2016**, *22*, 869-873.

[7] a) A. V. Lunchev, V. C. Hendrata, A. Jaggi, S. A. Morris, R. Ganguly, X. Chen, H. Sun, A. C. Grimsdale, *J. Mater. Chem. C* **2018**, *6*, 3715-3721; b) A. V. Lunchev, S. A. Morris, R. Ganguly, A. C. Grimsdale, *Chem. –Eur. J.* **2019**, *25*, 1819-1823.

[8] D. Hellwinkel, P. Ittemann, *Liebigs Ann. Chem.* **1985**, *1985*, 1501-1507.

[9] S.-P. Luo, N.-Y. Chen, Y.-Y. Sun, L.-M. Xia, Z.-C. Wu, H. Junge, M. Beller, Q.-A. Wu, *Dyes Pigm.* **2016**, *134*, 580-585.

[10] a) J. Marco-Contelles, E. Pérez-Mayoral, A. Samadi, M. d. C. Carreiras, E. Soriano, *Chem. Rev.* **2009**, *109*, 2652-2671; b) S. Gladiali, G. Chelucci, M. S. Mudadu, M.-A. Gastaut, R. P. Thummel, *J. Org. Chem.* **2001**, *66*, 400-405.

[11] T. Chanda, R. K. Verma, M. S. Singh, *Chem. –Asian. J.* **2012**, *7*, 778-787.

[12] V. Sridharan, P. Ribelles, M. T. Ramos, J. C. Menéndez, *J. Org. Chem.* **2009**, *74*, 5715-5718.

[13] a) S. Kumar, N. L. Agarwal, *J. Org. Chem.* **1986**, *51*, 2445-2449; b) S. K. Dubey, S. Kumar, *J. Org. Chem.* **1986**, *51*, 3407-3412; c) S. K. Balani, I. N. Brannigan, D. R. Boyd, N. D. Sharma, F. Hempenstall, A. Smith, *J. Chem. Soc., Perkin Trans. 1* **2001**, 1091-1097; d) K. Tanemura, T. Suzuki, Y. Nishida, K. Satsumabayashi, T. Horaguchi, *Chem. Commun.* **2004**, 470-471.

[14] a) K. Chandraprakash, N. Vandana, M. Sankaran, C. Uvarani, A. Ata, P. S. Mohan, T. Suresh, *J. Heterocycl. Chem.* **2018**, *55*, 2766-2771; b) M. Barbero, S. Bazzi, S. Cadamuro, S. Dughera, *Tetrahedron Lett.* **2010**, *51*, 2342-2344; c) P. Sarma, A. K. Dutta, P. Gogoi, B. Sarma, R. Borah, *Monatsh. Chem.* **2015**, 146, 173-180; d) M. A. Nasseri, S. A. Alavi, M. Kazemnejadi, A. Allahresani, *ChemistrySelect* **2019**, *4*, 8493-8499.

[15] a) Y. Zou, D. D. Young, A. Cruz-Montanez, A. Deiters, *Org. Lett.* **2008**, *10*, 4661-4664; b) L. Zhou, K. Nakajima, K.-i. Kanno, T. Takahashi, *Tetrahedron Lett.* **2009**, *50*, 2722-2726; c) T. Takahashi, S. Li, W. Huang, F. Kong, K. Nakajima, B. Shen, T. Ohe, K.-i. Kanno, *J. Org. Chem.* **2006**, *71*, 7967-7977; d) S. Li, H. Qu, L. Zhou, K.-i. Kanno, Q. Guo, B. Shen, T. Takahashi, *Org. Lett.* **2009**, *11*, 3318-3321.

[16] S. Tamura, S. Inomata, M. Ebine, T. Genji, I. Iwakura, M. Mukai, M. Shoji, T. Sugai, M. Ueda, *Bioorg. Med. Chem. Lett.* **2013**, *23*, 188-193.

[17] a) C. Fontenas, E. Bejan, H. A. Haddou, G. G. A. Balavoine, *Synth. Commun.* **1995**, *25*, 629-633; b) S. Kaiser, S. P. Smidt, A. Pfaltz, *Angew. Chem. Int. Ed.* **2006**, *45*, 5194-5197.

[18] C. M. Cardona, W. Li, A. E. Kaifer, D. Stockdale, G. C. Bazan, *Adv. Mater.* **2011**, *23*, 2367-2371.

[19] D. Tzalis, Y. Tor, *Tetrahedron Lett.* **1995**, *36*, 6017-6020.

[20] G. Accorsi, A. Listorti, K. Yoosaf, N. Armaroli, *Chem. Soc. Rev.* **2009**, *38*, 1690-1700.

[21] a) D. R. Maulding, B. G. Roberts, *J. Org. Chem.* **1969**, *34*, 1734-1736; b) M. T. Miller, T. B. Karpishin, *Inorg. Chem.* **1999**, *38*, 5246-5249.

[22] W. A. W. Jr., E. C. Lim, *J. Chem. Phys.* **1978**, *68*, 433-454.
[23] A. Airinei, R. Tigoianu, R. Danac, C. M. Al Matarneh, D. L. Isac, *J. Lumin.* **2018**, *199*, 6-12.
[24] R. Aliveisi, A. Taherpour, I. Yavari, *Polycyclic Aromat. Compd.* **2019**, *39*, 462-469.
[25] Y. Yang, W. Dai, Y. Zhang, J. L. Petersen, K. K. Wang, *Tetrahedron* **2006**, *62*, 4364-4371.
[26] O. Baudoin, M. P. Teulade-Fichou, J. P. Vigneron, J. M. Lehn, *J. Org. Chem.* **1997**, *62*, 5458-5470.
[27] T. Yamamoto, Y. Saitoh, K. Anzai, H. Fukumoto, T. Yasuda, Y. Fujiwara, C. Byoung-Ki, K.,Kenji T. Miyamae, *Macromolecules* **2003**, *36*, 6722-6729.
[28] R. J. Lakowicz, *Principles of Fluorescence Spectroscopy,* Springer Science+Business Media, **2006**, Chapter 6.
[29] J. Pina, J. Seixas de Melo, F. Pina, C. Lodeiro, J. C. Lima, A. J. Parola. *Inorg. Chem.* **2005**, *44*, 7449-7458.
[30] H. Liu, Y. Peng, Y. Zhang, X. Yang, F. Feng, X. Luo, L. Yan, B. Hu, W. Huang. *Dyes Pigm.* **2020**, *174*, 108074.
[31] K. Hayashi, H. Akutsu, H. Ozaki, H. Sawai, *Chem. Commun.* **2004**, *40*, 1386-1387.

Table of Contents

Synthesis, Optical and Electrochemical Properties of Isomeric Dibenzophenanthroline Derivatives

Animesh Ghosh, Tianjiao Li, Wenjun Ni, Tong Wu, Caihong Liang, Maja Budanovic, Samuel A. Morris, Maciej Klein, Richard D. Webster, Gagik G. Gurzadyan,* and Andrew C. Grimsdale*

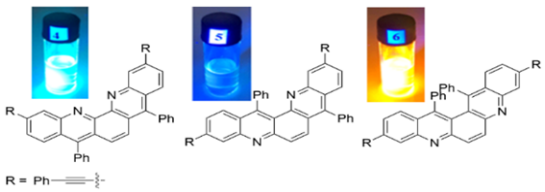

Isomeric dibenzo-1,10-, 1,7- and 4,7-phenathroline derivatives (DBPs) were made using Friedländer condensations and their optical and electrochemical properties compared. They possessed similar LUMO energies but the 4,7-DBPs had higher HOMO energies. The 1,7-DBPs showed strongly quenched emission compared to 1,10-DBPs due to charge transfer. The PL emission of 4,7-DBPs was enhanced by excimer formation, but their photostability was reduced. Bis(phenylethynyl) substituted DBPs showed enhanced solubility and luminescence compared to the parent compounds.